Journal of Fluorescence (2021) 31:237–246
https://doi.org/10.1007/s10895-020-02653-5

ORIGINAL ARTICLE

A Highly Selective and Sensitive Peptide-Based Fluorescent Ratio Sensor for Ag^+

Shuaibing Yu[1] · Zhaolu Wang[1] · Lei Gao[2] · Bo Zhang[1] · Lei Wang[1] · Jinming Kong[3] · Lianzhi Li[1]

Received: 13 August 2020 / Accepted: 12 November 2020 / Published online: 20 November 2020

Abstract

A fluorescence ratio sensor based on dansyl-peptide, Dansyl-Glu-Cys-Glu-Glu-Trp-NH_2 (D-P5), was efficiently synthesized by Fmoc solid phase peptide synthesis. The sensor exhibits high selectivity and sensitivity for Ag^+ over 16 metal ions in 100 mM sodium perchlorate and 50 mM 2-[4-(2-hydroxyethyl)piperazin-1-yl]ethanesulfonic acid buffer solution by fluorescence resonance energy transfer. The 1:1 binding stoichiometry of the sensor and Ag^+ is measured by fluorescence ratio response and the job's plot. The dissociation constant of the sensor with Ag^+ was calculated to be 6.4×10^{-9} M, which indicates that the sensor has an effective binding affinity for Ag^+. In addition, the limit of detection of the sensor for Ag^+ was determined to be 80 nM, which also indicates that the sensor has a high sensitivity to Ag^+. Result showed that the sensor is an excellent Ag^+ sensor under neutral condition. Furthermore, this sensor displays good practicality for Ag^+ detection in river water samples without performing tedious sample pretreatment, as well as for silver chloride detection.

Keywords Fluorescence ratio sensor · Peptide · Ag^+ · Fluorescence resonance energy transfer

Introduction

Silver is a very important metal which is widely used in electrical industry, photographic materials and medical applications. Silver itself has good electrical and thermal conductivity as an electronic material, silver halide can be used as a photosensitive material, and silver ion and silver-containing compounds can kill or inhibit bacteria and viruses [1–3]. On the other hand, due to the non-biodegradability of heavy metals and transition metals, it will accumulate in the environment and organisms [4]. Long-term accumulation of these metals can cause a series of hazards to the environment and organisms [5–9]. Silver ion is considered to be harmful substance and is also a major environmental pollutant. Moreover, it can damage enzymes and combine with amines and various metabolites, posing a threat to environmental safety and human health [10, 11]. Therefore, a fast and sensitive method for detecting Ag^+ is needed.

Standard method for detection of silver in water, such as inductively coupled plasma-mass spectrometry (ICP-MS) [12], is a complicated and time-consuming procedure. Compared with other detection methods, fluorescence detection has many advantages such as good selectivity, high sensitivity, fast response, low detection limit and strong anti-interference ability [13–21]. Many fluorescent chemical sensors for transition metal ion (HTM) and heavy metal detection have been reported [22–28], and significant achievements have been made in immunoassay, drug analysis and environmental pollution monitoring and so on [29–41]. Peptide is a kind of biomolecule existing in nature [42], it is formed by the dehydration and condensation of amino acids. Therefore, there are many sites that can chelate metal ions with multiple coordination [43], which provide strong and fast binding ability. At the same time, due to the difference of the sequence of amino acids, the structures of peptides are also different, so the selectivity of peptide to metal ion can be optimized by adjusting the sequence of amino acids [44], thereby achieving high

✉ Lianzhi Li
lilianzhi1963@163.com

[1] School of Chemistry and Chemical Engineering, Liaocheng University, Liaocheng 252059, People's Republic of China

[2] Zhong Yuan Academy of Biological Medicine, Liaocheng People's Hospital Affiliated to Shandong University, Liaocheng 252000, People's Republic of China

[3] School of Environmental and Biological Engineering, Nanjing University of Science and Technology, Nanjing 210094, People's Republic of China

sensitivity and selectivity [45–47]. By optimizing the sequence of peptide, the selectivity and sensitivity of the sensor to metal ion can be improved, which makes the peptide-based chemical sensor to be effective in detection of heavy metal ions. Currently, comparing with other metal ions, few methods for detecting silver ion have been reported [48–57]. Therefore, we have done some researches on this aspect and reported several peptide-based sensors for the detection of Hg^{2+}, Cu^{2+} and Cd^{2+} [33, 34, 41–44]. As a part of this series of research work, herein we synthesized the Dansyl-Glu-Cys-Glu-Glu-Trp-NH_2 as a sensor because it contains cysteine (Cys) and glutamic acid (Glu). Cys containing sulfydryl group and Glu containing carboxyl group can interact with several heavy metal ions such as Ag^+, Cu^{2+}, Zn^{2+} and Hg^{2+}. Based on the principle of fluorescence resonance energy transfer (FRET) effect, D-P5 can effectively detect Ag^+ by fluorescence ratio response. Scheme 1 is the proposed fluorescence detection mode of D-P5 for Ag^+. This sensor could have some practical applications in the environmental and biological fields.

Experimental

Materials and Instruments

Fmoc-L-Glu(OtBu)-OH, Fmoc-L-Cys(Trt)-OH, Fmoc-L-Trp(Boc)-OH and Rink amide resin were bought from CS Bio. Co., USA. Dansyl chloride and trifluoroacetic acid (TFA) were from Shanghai Macklin Biochemical Co., Ltd. Thioanisole, N,N-diisopropylethylamine (DIEA), N,N′-diisopropylcarbodiimide (DIC) and 2-(1H-benzotriazole-1-yl)-1,1,3,3-tetramethyluronium hexafluorophosphate (HBTU) were obtained from Shanghai GL Biochem Ltd. The solutions of different metal ions with concentration of 10 mM were prepared from NaCl, KCl, $BaCl_2$, $CrCl_3$, $MnCl_2$, $CoCl_2$, $NiCl_2$, $ZnCl_2$, $CdCl_2$, $HgCl_2$, $CuSO_4$, $Mg(NO_3)_2$, $Al(NO_3)_3$, $AgNO_3$, $Pb(NO_3)_2$ and $Fe(NO_3)_3$ in distilled water. All the solutions used were prepared in 100 mM $NaClO_4$, 50 mM 2-[4-(2-hydroxyethyl)piperazin-1-yl]ethanesulfonic acid (HEPES) buffer solution at pH = 7.0.

CS 136 Peptide Synthesizer (CS Bio Co., USA), CR22G high speed refrigerated centrifuge (Japan), API 4500 QTRAP

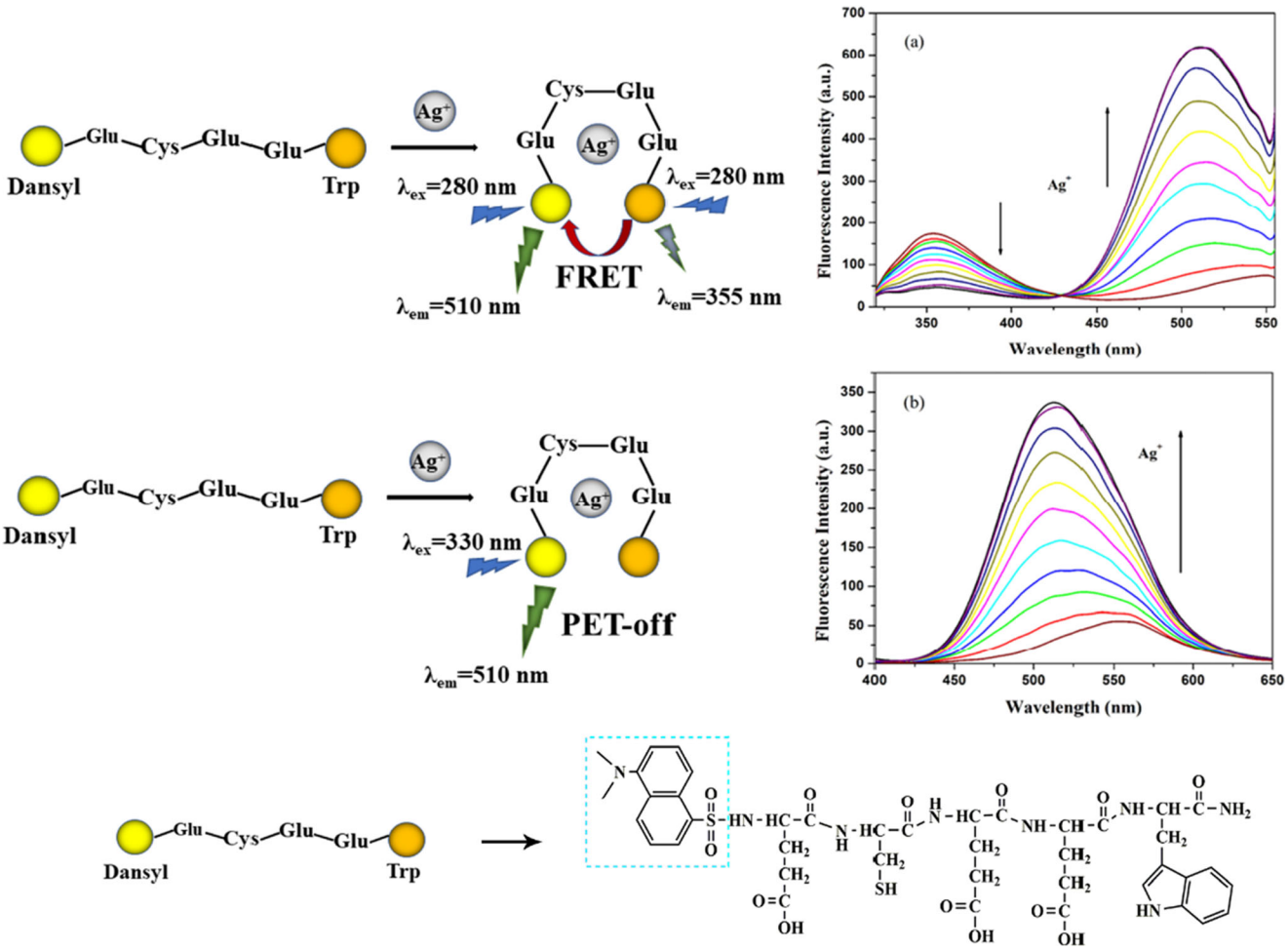

Scheme 1 Proposed fluorescence ratio detection mode of the sensor for Ag^+

Mass Spectrometer (Applied Biosystems/MDS SCIEX, USA), Hitachi F-7000 fluorescence spectrofluorometer (Hitachi Inc., Japan).

Synthesis of the Sensor

The synthesis of D-P5 was performed on a CS136 solid phase peptide synthesizer by using standard Fmoc solid-phase peptide synthesis method. Fmoc-Trp(Boc)-OH (0.6 mmol) was assembled on Rink Amide resin (0.2 mmol). When the Fmoc group was deprotected from the resin bound Trp, Fmoc-Glu(OtBu)-OH (0.6 mmol), Fmoc-Glu(OtBu)-OH (0.6 mmol), Fmoc-Cys(Trt)-OH (0.6 mmol) and Fmoc-Glu(OtBu)-OH (0.6 mmol) were successively assembled. Then, the solution of dansyl chloride (0.6 mmol) of DMF was added to the resin bound to pentapeptide. After all amino acid couplings were finished, the resultant resin was washed with anhydrous methanol and dried under vacuum. Then, the peptide was cleaved from the Rink Amide resin by treatment with a mixture of 6 mL TFA:thioanisole:phenol:H_2O:EDT (82.5:5:5:5:2.5, *v*/v/v/v/v) at room temperature for 4 h [58]. Finally, the peptide was extracted in ether at −20 °C and centrifuged at 10000 rpm for 5 min at −4 °C. The resulting product D-P5 was characterized by ESI mass spectrometry in positive ion mode.

General Fluorescence Measurements

A stock solution of 3.0 mM D-P5 was prepared in 100 mM $NaClO_4$, 50 mM HEPES buffer, pH 7.0. Fluorescence spectra were measured in a buffer containing 100 mM $NaClO_4$, 50 mM HEPES at pH = 7.0 using a Hitachi F-7000 fluorescence spectrofluorometer. Emission spectra of the sensor in the presence of various metal ions (K^+, Na^+, Ba^{2+}, Mn^{2+}, Cr^{3+}, Co^{2+}, Ni^{2+}, Zn^{2+}, Cd^{2+} and Hg^{2+} as chloride salts, Mg^{2+}, Al^{3+}, Ag^+, Pb^{2+} and Fe^{3+} as nitrate salts, Cu^{2+} as sulfate salts) were measured by excitation with 280 nm and 330 nm wavelengths, respectively. Excitation and emission slits were 5 nm and 10 nm, respectively, and the scanning speed was 300 nm·min^{-1}.

Fluorescence emission spectra of D-P5 and D-P5-Ag system were determined at various pH values with excitation wavelength of 280 nm. The pH values of the sample solutions were adjusted by addition of different amounts of $HClO_4$ or NaOH solutions.

Binding Stoichiometry, Dissociation Constant (K_d) and Limit of Detection

The Job's plot was used to determine the binding stoichiometry of D-P5 with Ag^+ ion. The fluorescence measurement for Job's plot was performed in 100 mM $NaClO_4$, 50 mM HEPES buffer solution at pH = 7.0. The D-P5 concentration gradually decreased, while Ag^+ concentration increased gradually, and the total concentration of D-P5 and Ag^+ was 20 μM.

The dissociation constant could be calculated by the non-linear least squares fitting of the data with the following equation [36].

$$F = F_{max} \times \frac{([D] + [x] + K_d) - \sqrt{([D] + [x] + K_d)^2 - 4[D][x]}}{2[D]}$$

where F is the fluorescence signal of D-P5 in the presence of the relative Ag^+ concentration, and F_{max} is the final fluorescence signal, $[D]$ and $[x]$ are the total concentration of peptide (D-P5) and metal ion (Ag^+), respectively. K_d is the dissociation constant.

The measurement of limit of detection (LOD) is based on the titration curve of D-P5 with Ag^+. The fluorescence spectra of D-P5 were performed ten times and then the standard deviation of the blank was measured. The fluorescence signal corresponding to different Ag^+ concentrations was linearly fitted to the plot of Ag^+ concentration to obtain a slope. The limit of detection was calculated by the equation:

$$LOD = 3SD/m,$$

where SD is the relative standard deviation of the blank and m is the slope of the line.

Results and Dicussion

Solid Phase Synthesis of the Sensor

The success of the synthesis was confirmed by ESI mass spectrometer (Fig. 1). ESI mass of D-P5 was calculated as 927.3 [M + H^+]. Since D-P5 contains multiple carboxyl groups, it is possible to take off H^+ and combine with Na^+, K^+, NH_4^+ ions. It was observed that peaks at 927.1 can be assigned as [M + H^+]$^+$, 971.3 as [(M-2H^+) + 2Na^++H^+]$^+$ and 983.4 as [(M-3H^+) + Na^++2NH_4^++H^+]$^+$ (Fig. 1a). The ESI-MS results of D-P5-Ag showed the occurrence of peak 1089.4, corresponding to [(M-3H^+) + Ag^++K^++NH_4^++H^+]$^+$ (Fig. 1b). These results confirmed that D-P5 could bind Ag^+ in the ratio of 1:1.

Fluorescence Spectra

The selective detection ability of D-P5 for metal ion was studied by fluorescence spectra in the presence of 16 metal ions including Cd^{2+}, Co^{2+}, Zn^{2+}, Hg^{2+}, Mn^{2+}, Ni^{2+}, Cr^{3+}, Ba^{2+}, K^+, Na^+, Al^{3+}, Pb^{2+}, Mg^{2+}, Ag^+, Cu^{2+} and Fe^{3+} in 100 mM $NaClO_4$, 50 mM HEPES buffer at pH = 7.0 with excitation of 280 nm and 330 nm, respectively. The excitation wavelength at 280 nm was employed for monitoring both the Trp and dansyl

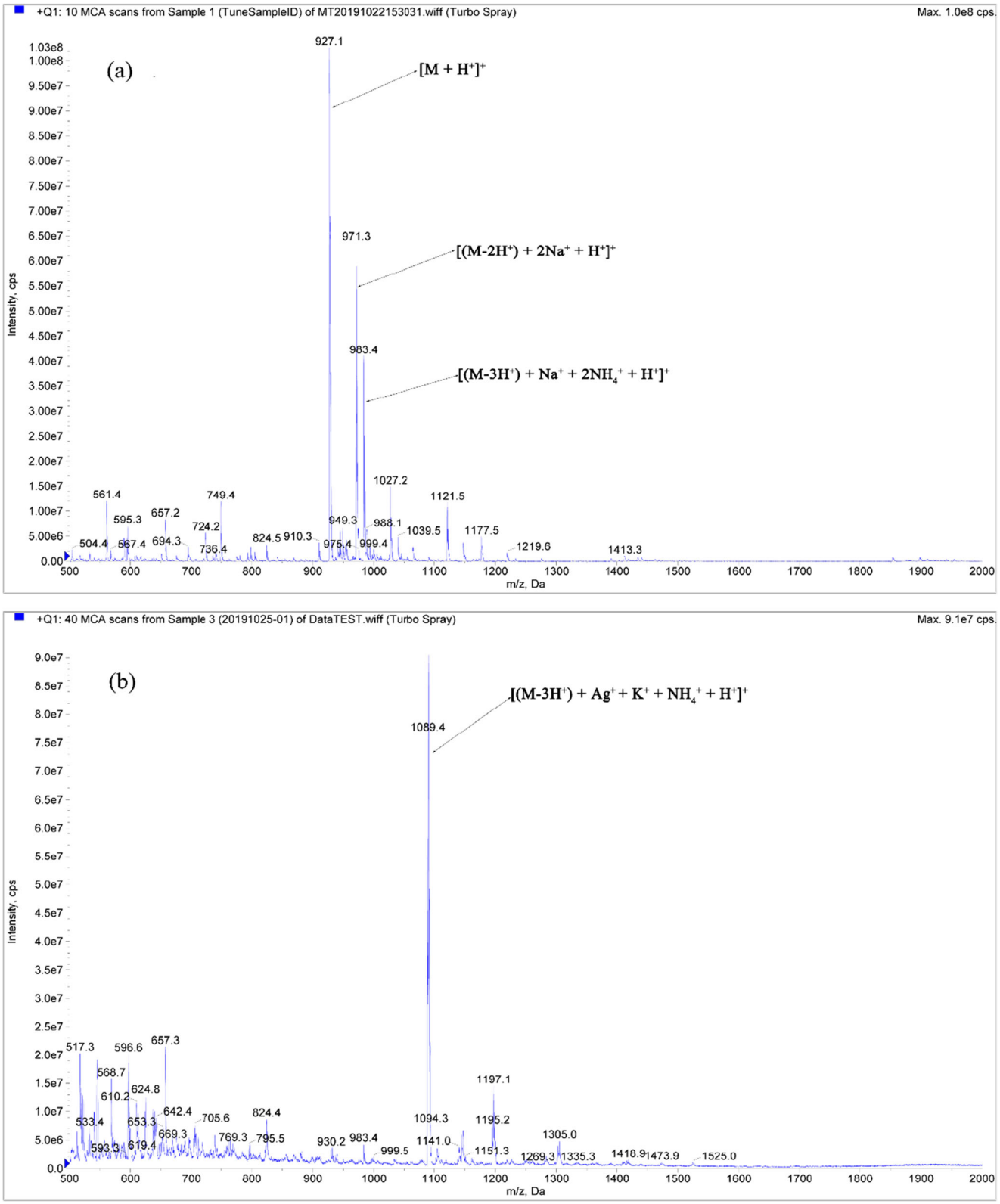

Fig. 1 ESI mass spectrum of D-P5 (10.0 μM) (a) and D-P5-Ag (10.0 μM) (b) in ethanol:water ($EtOH:H_2O$) (1:1) solutions

fluorophore emissions, while 330 nm was used only for monitoring the dansyl fluorophore emission. Figure 2 shows the fluorescence response of D-P5 in the absence and presence of different metal ions with excitation wavelength of 280 nm and 330 nm. As shown in Fig. 2a, only the addition of Ag^+ caused the significant decrease of fluorescence signal at 355 nm and

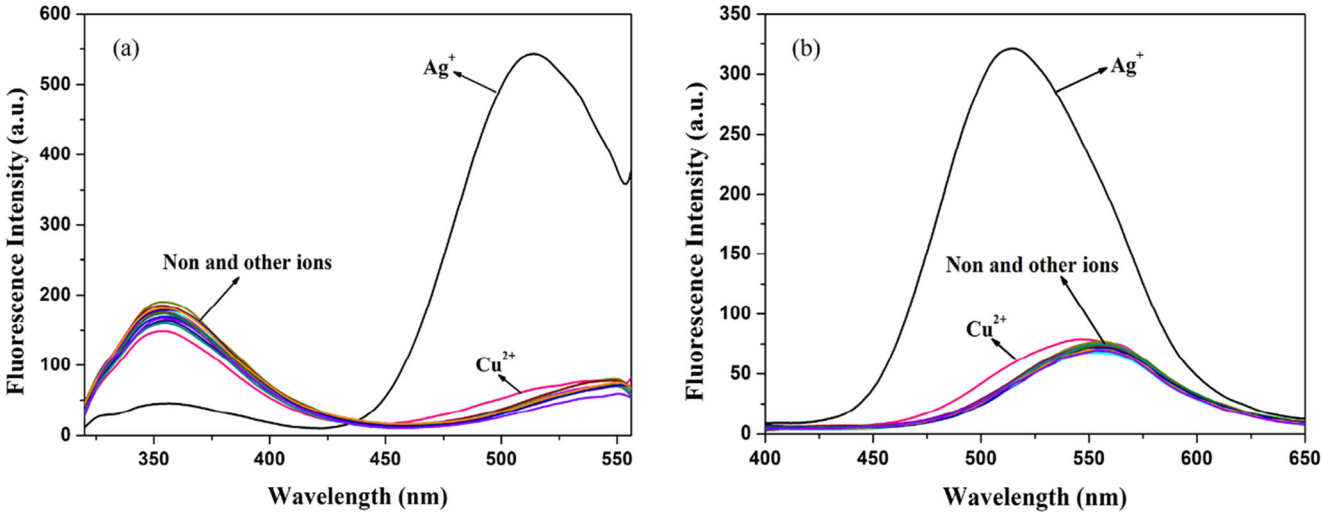

Fig. 2 Fluorescence spectra of the sensor (10.0 μM) in the absence and presence of 16 different metal ions (10.0 μM) at λ_{ex} = 280 nm (a) and λ_{ex} = 330 nm (b)

significant increase of fluorescence signal at 550 nm with a concomitant blue shift to 510 nm, while the addition of other metal ions only caused a slight fluorescence signal decrease of the D-P5. Hence, the addition of Ag^+ leads to a fluorescence signal decrease of Trp group and fluorescence signal increase of dansyl fluorescent group. When excited at 330 nm, D-P5 has a maximum emission peak at 550 nm. In the presence of different metal ions, only Ag^+ induced a strong fluorescence enhancement with a 40 nm blue shift from 550 nm to 510 nm (Fig. 2b). The fluorescence spectrum of dansyl group is very sensitive to the change of its microenvironment [59]. The fluorescence quenching of dansyl group may be due to photoinduced electron transfer (PET) from the amino acid residues of peptide chain to the dansyl fluorophore, leading to a turn-off response, but its fluorescence property is then recovered when D-P5 coordinates to Ag^+ [60]. The result thus showed that D-P5 has a high selectivity to Ag^+.

The selectivity of D-P5 to metal ion is also reflected by the fluorescence ratio (F_{510}/F_{355}) histogram excited at 280 nm. Figure 3 shows the fluorescence ratio (F_{510}/F_{355}) of D-P5 in the presence of different metal ions. After adding the same concentration of Pb^{2+}, Cd^{2+}, Mn^{2+}, Al^{3+}, Cr^{3+}, Ni^{2+}, Mg^{2+}, Ba^{2+}, Zn^{2+}, Co^{2+}, Na^+, K^+, Hg^{2+}, Cu^{2+} and Fe^{3+} ions to D-P5 solutions, the fluorescence ratio (F_{510}/F_{355}) of D-P5 did not change significantly. Meanwhile, the free D-P5 (1.0 mM) displayed a yellow fluorescence under 365 nm UV lamp excitation. Upon the addition of various metal ions (1.0 mM) to D-P5 solutions, it showed high selectivity for Ag^+ (1.0 mM) in a "turn-on" mode with the fluorescence colour change from yellow to green under 365 nm UV lamp excitation. This indicates that the interference of these ions on the detection of Ag^+ by the D-P5 is negligible.

There are a large amount of alkali and alkaline earth metal ions in environmental and biological organisms. Therefore, the effects of these alkali and alkaline earth metals on the fluorescence spectra of D-P5 and D-P5-Ag solutions were studied. As shown in Fig. 4a, when the concentrations of these metal ions are 1000 times those of Ag^+, the fluorescence emission signal of D-P5-Ag system is not significantly affected. This result indicates that both alkali and alkaline earth metals have little interference on the detection of Ag^+.

Similarly, for investigating the effects of different anions on the fluorescence property of the system, the fluorescence spectra of D-P5 and D-P5-Ag in the presence of different anions were measured under the same conditions. As shown in Fig. 4b, when adding sodium salts consisting of different anion to the D-P5-Ag solution and the concentrations of these salts reached 1000 times those of D-P5-Ag, there were no obvious effects on the fluorescence ratio (F_{510}/F_{355}) of D-P5 and D-P5-Ag. The change indicates that these anions have little interference with the detection of Ag^+.

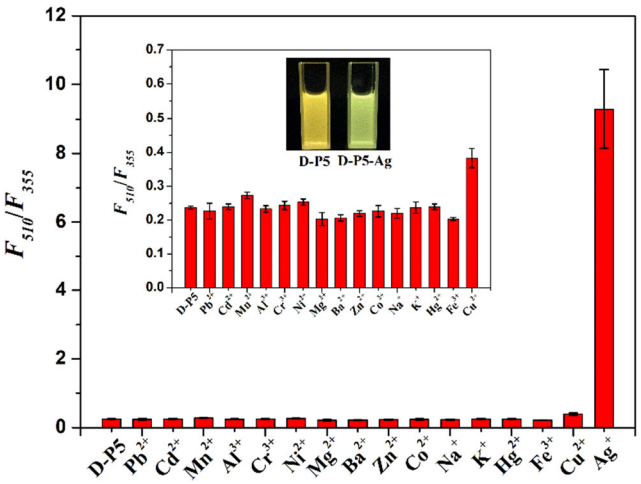

Fig. 3 Fluorescence ratio (F_{510}/F_{355}) histogram of the sensor upon the addition of 16 different metal ions. Insets were the colors of D-P5 (1.0 mM, yellow) and D-P5-Ag (1.0 mM, green) under 365 nm ultraviolet lamp excitation

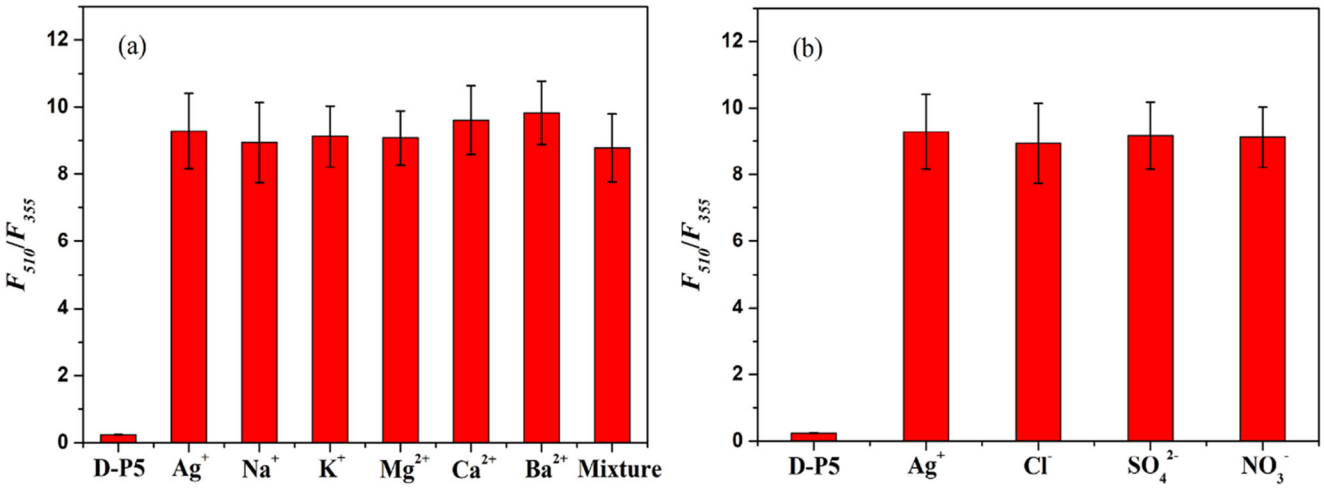

Fig. 4 (a) Fluorescence ratio (F_{510}/F_{355}) histogram of D-P5-Ag (10.0 μM) in the presence of different alkali metal and alkaline earth metal ions. (b) Fluorescence ratio (F_{510}/F_{355}) histogram of D-P5-Ag (10.0 μM) in the presence of different anions

Fluorescent titration spectra of D-P5 with varying concentrations of Ag^+ in 50 mM HEPES buffer at pH = 7.0 with excitation of 280 nm are shown in Fig. 5a. When excited at 280 nm, the fluorescence emissions of the Trp group and dansyl group were observed. As Ag^+ concentration increased from 1.0 to 10.0 μM, the fluorescence signal at 355 nm gradually weakened, while the fluorescence signal at 550 nm gradually increased with a blue shifted to 510 nm. While excited at 330 nm, the fluorescence signal of D-P5 at 550 nm continuously increased with the addition of Ag^+, and a 40 nm blue shift from 550 to 510 nm of the maximum fluorescence peak occurred (Fig. 5b).

The phenomenon that occurs after the addition of Ag^+ is because the folding of D-P5 in the presence of Ag^+ brings the Trp group and the dansyl group closer, thereby generating fluorescence resonance energy transfer (FRET) from the Trp group to the dansyl group. To further verify the FRET mechanism, we quantitatively compared the two fluorescence signal increments at 510 nm of dansyl group under excitation of 280 nm and 330 nm in the presence of the same concentrations of Ag^+. In the presence of the same concentrations of Ag^+, the fluorescence signal increments of dansyl under 280 nm excitation were much bigger than those under 330 nm excitation (Fig. 6). Combining with the result of decrease of fluorescence signal at 355 nm of Trp group under excitation of 280 nm, it can be concluded that it occurred a FRET from the Trp group to the dansyl group.

The D-P5 system showed a high Ag^+ selectivity and FRET effect. D-P5 (Dansyl-Glu-Cys-Glu-Glu-Trp-NH_2) consists of cysteine (Cys) and glutamic acid (Glu) residues, sulfhydryl (-SH) of Cys and carboxyl (-COO^-) of Glu can interact with Ag^+. The property of that D-P5 selectively binds to Ag^+ ion but not to other ions is attributed to both of the natures of Ag^+ and the amino acid composition and specific sequence of D-

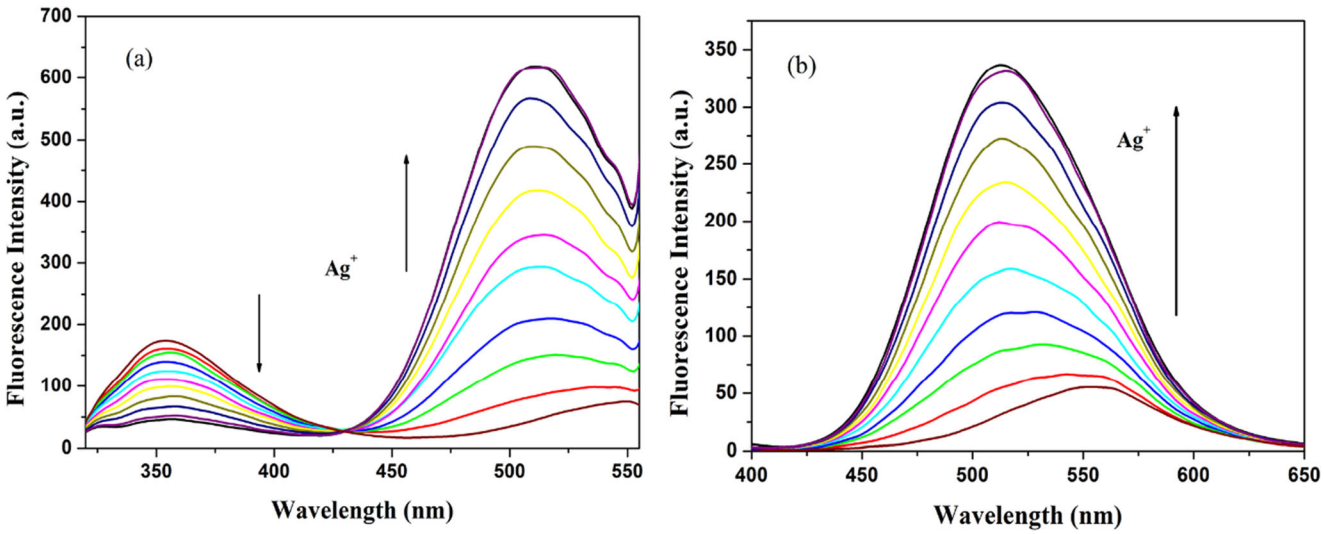

Fig. 5 Fluorescence spectra of the sensor (10.0 μM) in the presence of different concentrations of Ag^+ at λ_{ex} = 280 nm (a) and λ_{ex} = 330 nm (b)

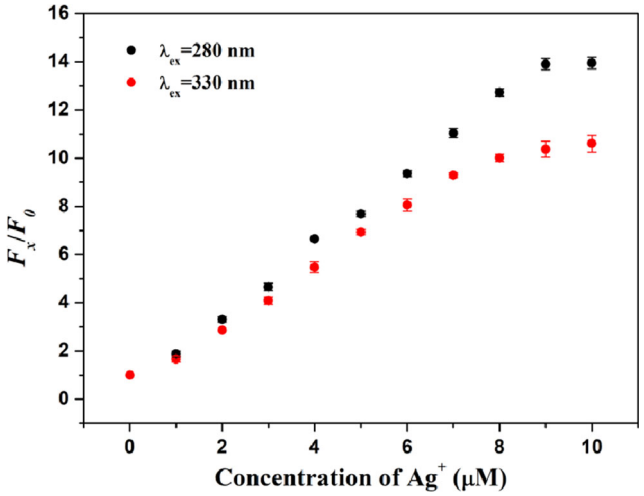

Fig. 6 The ratios (F_x/F_0) of fluorescence intensity at 510 nm of dansyl group under excitation of 280 nm and 330 nm in the presence of the same concentrations of Ag^+

P5. The binding of D-P5 with Ag^+ shortens the distance between Trp (fluorescent donor) and dansyl (fluorescent receptor), resulting in a FRET effect. However, D-P5 can hardly bind to other metal ions due to the nature of its nature, hence other metal ions can't make it FRET.

pH Effect

The effect of pH value on the fluorescence spectra of D-P5 and D-P5-Ag solutions were studied. As shown in Fig. 7a, the fluorescence ratio (F_{510}/F_{355}) of D-P5 hardly changed with the pH value changed from 1 to 12, so the effect of pH on the fluorescence ratio of D-P5 is not very obvious. When the pH was lower than 4, the fluorescence ratio of D-P5-Ag was weak, indicating that the interaction between Ag^+ and D-P5 is weak in acidic condition. When the pH was between 4 and 7, the fluorescence ratio F_{510}/F_{355} of D-P5-Ag increased. This

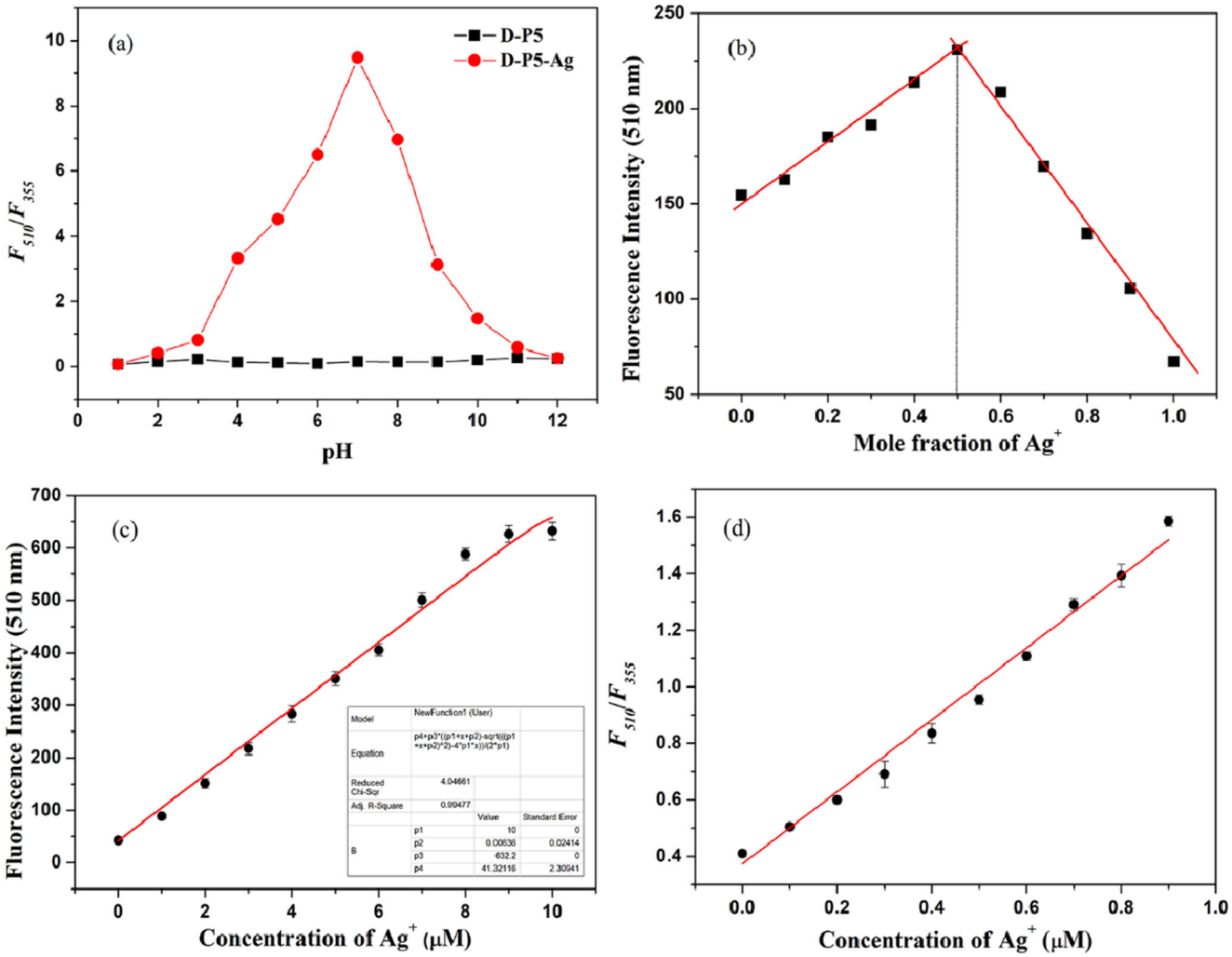

Fig. 7 (a) Fluorescence ratio (F_{510}/F_{355}) of D-P5 (10.0 μM) and D-P5-Ag (10.0 μM) at different pH; (b) Job's plot for determining the stoichiometry of D-P5 with Ag^+; (c) The nonlinear least squares curve fitting for the determination of dissociation constant of the sensor with Ag^+; (d) Fluorescence ratio (F_{510}/F_{355}) of the sensor (10.0 μM) as a function of Ag^+ concentration for the measurement of limit of determination

Table 1 Various methods for detecting Ag^+

Detection agent	LOD/ (nM)	Reference
ssDNA/nano-graphite	0.3	10
Monolayer g-C_3N_4	52.3	11
OS-g-C_3N_4-dots	2	49
Dithiourea-appended 1,8-naphthalimide	1200	51
AuNPs-Tris	410	52
Single-cytosine	0.02	53
Graphene quantum dots and o-phenylenediamine	250	54
Glutathione-mediated MnO_2 nanosheets	4.23	55
Rose Bengal dye	98	56
Heptamethine cyanine dye	30	57
D-P5	80	This work

indicates that D-P5 can strongly bind to Ag^+ at this pH range, hence the FRET effect is significantly enhanced. This is due to the deprotonation of the side chain -SH group of the Cys residue which increases the negative charge [61]. When pH > 8, Ag^+ was prone to hydrolysis reaction, which reduces its binding ability to D-P5. When pH = 7, the fluorescence ratio F_{510}/F_{355} reached a maximum, indicating that D-P5 is optimal for Ag^+ detection in the neutral state.

Binding Stoichiometry, Dissociation Constant (K_d) and Detection Limit

Figure 7b is the Job's plot of the fluorescence signal for D-P5 and Ag^+ solutions. The binding stoichiometry can be obtained from this plot. It indicated that a 1:1 binding was obtained between D-P5 and Ag^+ in 50 mM HEPES solution. The dissociation constant of D-P5 with Ag^+ was calculated to be 6.4×10^{-9} M ($R^2 = 0.9948$) from the non-linear least squares fitting of the data with the equation in the reference, which indicated that D-P5 has a strong binding affinity to Ag^+ (Fig. 7c).

The limit of detection of D-P5 for Ag^+ could be calculated by the linear relationship between the fluorescence ratio (F_{510}/F_{355}) and Ag^+ (Fig. 7d). The detection limit of 80 nM is obtained by the formula $LOD = 3SD/m$ ($R^2 = 0.9894$). The detection limit for Ag(I) (80 nM) was much lower than the EPA's drinking water maximum contaminant level of Ag^+ (0.1 mg/L) [62]. Table 1 gives some methods for detecting silver ion.

Table 2 Detection of Ag^+ in lake water

Water sample	[Ag^+] added (μM)	[Ag^+] found (μM)	Recovery (%)
1	1.0	1.07 ± 0.03	107.0 ± 3.0
2	2.0	2.32 ± 0.06	116.0 ± 3.0
3	3.0	3.48 ± 0.10	116.0 ± 4.0
4	4.0	4.24 ± 0.12	106.0 ± 3.0
5	5.0	4.84 ± 0.14	96.8 ± 2.8

Table 3 Detection of silver chloride in lake water

Water sample	[AgCl] added (μM)	[AgCl] found (μM)	Recovery (%)
1	2.0	2.04 ± 0.17	102.0 ± 8.5
2	4.0	4.14 ± 0.28	106.0 ± 7.0
3	6.0	5.73 ± 0.45	95.5 ± 7.5

Application for the Detection of Lake Water Samples

Based on the high selectivity and sensitivity of D-P5 to Ag^+, this sensor can be used for detecting Ag^+ in lake water samples. The standard curve is gained by adding $AgNO_3$ standard solution to distilled water. It can be seen from the fluorescence titration curve (Fig. S1) that there is a good linear relationship when the concentration of Ag^+ is in the range of 1.0–5.0 μM. Based on this result, we added $AgNO_3$ (1.0–5.0 μM) solutions to the lake samples and then detected their Ag^+ concentrations, the recovery rates were obtained in Table 2. Result indicated that D-P5 exhibits a good recovery for Ag^+. In addition, D-P5 can be also used for detecting Ag(I) existed in the form of silver chloride. As shown in Table 3, D-P5 shows a good recovery rate for AgCl, indicating that the binding of D-P5 to Ag^+ is much stronger than that of Cl^- to Ag^+. Therefore, the results showed that D-P5 has good potential application for environmental detection.

Conclusions

In summary, a new dansyl-based peptide fluorescence probe (D-P5) was synthesized. It exhibited a high selectivity, sensitivity and affinity for Ag^+ ion over other common metal ions in 100 mM $NaClO_4$, 50 mM HEPES solution. The sensor is based on FRET from tryptophan residue to dansyl group for Ag^+ detection with excitation wavelength of 280 nm. This D-P5 sensor had a low detection limit of 80 nM with a dissociation constant of 6.4×10^{-9} M. This fluorescent peptide sensor displayed good practicality for river water samples without performing tedious sample pretreatment. In addition, the effect on the fluorescence response under different pH conditions indicates that the detection of Ag^+ is more favourable under neutral conditions, which provides a basis for future application prospects in biological and environmental systems.

Supplementary Information The online version contains supplementary material available at https://doi.org/10.1007/s10895-020-02653-5.

Authors' Contributions Shuaibing Yu and Zhaolu Wang contributed equally. Methodology, Conceptualization, Investigation, Writing - original draft. Lei Gao: Investigation, Writing - original draft. Bo Zhang: Investigation. Lei Wang: Visualization, Project administration. Jinming Kong: Methodology, Writing - review & editing. Lianzhi Li: Resources, Supervision, Funding acquisition, Writing - review & editing.

Funding This work was supported by the Scientific Research Foundation of Liaocheng University, China (No. 318011919), and the National Natural Science Foundation of China (No. 21974068).

Data Availability The data used to support the findings of this study are included within the article.

Compliance with Ethical Standards

Conflict of Interest There are no conflicts to declare.

References

1. Calixto S, Ganzherli N, Gulyaev S, Figueroa-Gerstenmaier S (2018) Gelatin as a photosensitive material. Molecules 23:2064
2. Li CW, Li QL, Long XY, Li TT, Zhao JX, Zhang K, E SF, Zhang J, Li Z, Yao YG (2017) In situ generation of photosensitive silver halide for improving theconductivity of electrically conductive adhesives. ACS Appl Mater Inter 9:29047–29054
3. Fromm KM (2011) Give silver a shine. Nat Chem 3:178
4. Miao P, Tang YG, Wang L (2017) DNA modified Fe_3O_4@Au magnetic nanoparticles as selective probes for simultaneous detection of heavy metal ions. Acs Appl Mater Inter 93:3940–3947
5. Hashim MA, Mukhopadhyay S, Sahu JN, Sengupta BJ (2011) Remediation technologies for heavy metal contaminated groundwater. J Environ Manag 92:2355–2388
6. Carter KP, Young AM, Palmer AE (2014) Fluorescent sensors for measuring metal ions in living systems. Chem Rev 114:4564–4601
7. Qian XH, Xu ZC (2015) Fluorescence imaging of metal ions implicated in diseases. Chem Soc Rev 44:4487–4493
8. Zhang JF, Zhou Y, Yoon J, Kim JS (2011) Recent progress in fluorescent and colorimetric chemosensors for detection of precious metal ions (silver, gold and platinum ions). Chem Soc Rev 40: 3416–3429
9. Boonkitpatarakul K, Wang J, Niamnont N, Liu B, Mcdonald L, Pang Y, Sukwattanasinitt M (2016) Novel turn-on fluorescent sensors with mega stokes shifts for dual detection of Al^{3+} and Zn^{2+}. Acs Sens 1:144–150
10. Wei Y, Li BM, Wang X, Duan YX (2014) Magnified fluorescence detection of silver(I) ion in aqueous solutions by using nanographite-DNA hybrid and DNase I. Biosens Bioelectron 58:276–281
11. Cao YJ, Wu W, Wang S, Peng H, Hu XG, Yu Y (2016) Monolayer g-C_3N_4 fluorescent sensor for sensitive and selective colorimetric detection of silver ion from aqueous samples. J Fluoresc 26:739–744
12. US EPA (1994) "Method 200.8: Determination of trace elements in waters and wastes by inductively coupled plasma-mass spectrometry," Revision 5.4. Cincinnati, OH. https://www.epa.gov/esam/epa-method-2008-determination-trace-elements-waters-and-wastes-inductively-coupled-plasma-mass
13. Wan JJ, Duan WX, Chen K, Tao YD, Dang J, Zeng KH, Ge YS, Wu J, Liu D (2018) Selective and sensitive detection of Zn(II) ion using a simple peptide-based sensor. Sensor Actuat B-Chem 255: 49–56
14. Lin YC, Zheng YF, Guo YC, Yang YL, Li HB, Fang Y, Wang C (2018) Peptide-functionalized carbon dots for sensitive and selective Ca^{2+} detection. Sensor Actuat B-Chem 273:1654–1659
15. Xu JB, Liu N, Hao CW, Han QQ, Duan YL, Wu J (2019) A novel fluorescence "on-off-on" peptide-based chemosensor for imultaneous detection of Cu^{2+}, Ag^{+} and S^{2-}. Sensor Actuat B-Chem 280:129–137
16. Wang B, Li HW, Gao Y, Zhang HY, Wu YQ (2011) A multifunctional fluorescence probe for the detection of cations in aqueous solution: the versatility of probes based on peptides. J Fluoresc 21:1921–1931
17. Donadio G, Martino RD, Oliva R, Petraccone L, Vecchio PD, Luccia BD, Ricca E, Isticato R, Donato AD, Notomista E (2016) A new peptide-based fluorescent probe selective or zinc(II) and copper(II). J Mater Chem B 4:6979–6988
18. Wang P, Zhou DG, Chen B (2018) High selective and sensitive detection of Zn(II) using tetrapeptide-based dansyl fluorescent chemosensor and its application in cell imaging. Spectrochim Acta A 204:735–742
19. Wang C, Sun LL, Zhao Q (2019) A simple aptamer molecular beacon assay for rapid detection of aflatoxin B1. Chinese Chem Lett 30:1017–1020
20. Bayraktutan T (2020) Investigation of photophysical and binding properties of rose bengal dye on graphene oxide and polyethyleneimine-functionalized graphene oxide nanocomposites. Chem Pap 74:3017–3024
21. Bayraktutan T (2019) Molecular interaction between cationic polymer polyethyleneimine and rose bengal dye: a spectroscopic study. J Turk Chem Soc Sect A-Chem 6:311–318
22. Li G, Tao F, Liu Q, Wang L, Wei Z, Zhu F, Chen W, Sun H, Zhou Y (2016) A highly selective and reversible water-soluble polymer based-colorimetric chemosensor for rapid detection of Cu^{2+} in pure aqueous solution. New J Chem 40:4513–4518
23. Yue QL, Shen TF, Wang JT, Wang L, Xu SL, Li HB, Liu JF (2013) A reusable biosensor for detecting mercury(II) at the subpicomolar level based on "turn-on" resonance light scattering. Chem Commun 49:1750–1752
24. Shen TF, Yue QL, Jiang XX, Wang L, Xu SL, Li HB, Gu XH, Zhang SQ, Liu JF (2013) A reusable and sensitive biosensor for total mercury in canned fish based on fluorescence polarization. Talanta 117:81–86
25. Wang LJ, Jia LP, Ma RN, Jia WL, Wang HS (2017) A colorimetric assay for Hg^{2+} detection based on Hg^{2+}-induced hybridization chain reactions. Anal Methods 9:5121–5126
26. Zhang YF, Li R, Xue QW, Li HB, Liu JF (2015) Colorimetric determination of copper(II) using a polyamine-functionalized gold nanoparticle probe. Microchim Acta 182:1677–1683
27. Bayraktutan T, Gür B, Demirbas Ü (2020) Detection of Al^{3+} and Fe^{3+} ions with phthalocyanine merocyanine 540 dye-based fluorescence resonance energy transfer. Bull Kor Chem Soc 41:973–980
28. Bayraktutan T, Bayraktutan ÖF (2020) A novel turn on fluorescence sensor for determination enoxaparin, a low molecular weight heparin. J Fluoresc 30:1591–1599
29. Joshi BP, Lohani CR, Lee KH (2010) A highly sensitive and selective detection of Hg(II) in 100% aqueous solution with fluorescent labeled dimerized Cys residues. Org Biomol Chem 8:3220–3226
30. Yang MH, Lohani CR, Cho H, Lee KH (2011) A methionine-based turn-on chemical sensor for selectively monitoring Hg^{2+} ions in 100% aqueous solution. Org Biomol Chem 9:2350–2356
31. Wang P, Wu J, Liu LX, Zhou PP, Ge YS, Liu D, Liu WS, Tang Y (2015) A peptide-based fluorescent chemosensor for measuring

cadmium ions in aqueous solutions and live cells. Dalton Trans 44: 18057–18064
32. Chen HX, Zhang JJ, Liu XJ, Gao YM, Ye ZH, Li GX (2014) Colorimetric copper(II) ion sensor based on the conformational change of peptide immobilized onto the surface of gold nanoparticles. Anal Methods 6:2580–2585
33. Pang XL, Dong JF, Gao L, Wang L, Yu SB, Kong JM, Li LZ (2020) Dansyl-peptide dualfunctional fluorescent chemosensor for Hg^{2+} and biothiols. Dyes Pigments 173:107888
34. Pang XL, Wang L, Gao L, Feng HY, Kong JM, Li LZ (2019) Multifunctional peptide-based fluorescent chemosensor for detection of Hg^{2+}, Cu^{2+} and S^{2-} ions. Luminescence 34:585–594
35. Joshi BP, Lee KH (2008) Synthesis of highly selective fluorescent peptide probes for metal ions: tuning selective metal monitoring with secondary structure. Bioorg Med Chem 16:8501–8509
36. Joshi BP, Park JY, Lee KH (2014) Recyclable sensitive fluorimetric detection of specific metal ions using a functionalized PEG-PS resin with a fluorescent peptide sensor. Sensor Actuat B-Chem 191:122–129
37. In B, Hwang GW, Lee KH (2016) Highly sensitive and selective detection of Al(III) ions in aqueous buffered solution with fluorescent peptide-based sensor. Bioorg Med Chem Lett 26:4477–4482
38. Tamanini E, Katewa A, Sedger LM, Todd MH, Watkinson M (2009) A synthetically simple, click-generated cyclam-based zinc(II) sensor. Inorg Chem 48:319–324
39. Tang XL, Peng XH, Dou W, Mao J, Zheng JR, Qin WW, Liu WS, Chang J, Yao XJ (2008) Design of a semirigid molecule as a selective fluorescent chemosensor for recognition of Cd(II). Org Lett 10: 3653–3656
40. Liu ZP, Zhang CL, He WJ, Yang ZH, Gao X, Guo ZJ (2010) A highly sensitive ratiometric fluorescent probe for Cd^{2+} detection in aqueous solution and living cells. Chem Commun 46:6138–6140
41. Wang ZL, Feng HY, Li Y, Xu T, Xue ZC, Li LZ (2015) A high selective fluorescent ratio sensor for Cd^{2+} based on the interaction of peptide with metal ion. Chinese J Inorg Chem 31:1946–1952
42. Li Y, Li LZ, Pu XW, Ma GL, Wang EQ, Kong JM, Liu ZP, Liu YZ (2012) Synthesis of a ratiometric fluorescent peptide sensor for the highly selective detection of Cd^{2+}. Bioorg Med Chem 22:4014–4017
43. Pang XL, Gao L, Feng HY, Li XD, Kong JM, Li LZ (2018) A peptide-based multifunctional fluorescent probe for Cu^{2+}, Hg^{2+} and biothiols. New J Chem 42:15770–15777
44. Feng HY, Gao L, Ye XH, Wang L, Xue ZC, Kong JM, Li LZ (2017) Synthesis of a heptapeptide and its application in the detection of mercury(II) ion. Chem Res Chin Univ 33:155–159
45. Sfrazzettoa GT, Satrianoa C, Tomaselli GA, Rizzarelli E (2016) Synthetic fluorescent probes to map metallostasis and intracellular fate of zinc and copper. Coord Chem Rev 311:125–167
46. Wu JC, Zou Y, Li CY, Sicking W, Piantanida I, Yi T, Schmuck C (2012) A molecular peptide beacon for the ratiometric sensing of nucleic acids. J Am Chem Soc 134:1958–1961
47. Schwarzenbach G (1952) Der chelateffekt. Helv Chim Acta 35: 2344–2359
48. Xu G, Wang GF, He XP, Zhu YH, Chen L, Zhang XJ (2013) An ultrasensitive electrochemical method for detection of Ag^{+} based on cyclic amplification of exonuclease III activity on cytosine-Ag^{+}-cytosine. Analyst 138:6900–6906
49. Wang HY, Lu QJ, Li MX, Li H, Liu YL, Li HT, Zhang YY, Yao SZ (2018) Electrochemically prepared oxygen and sulfur co-doped graphitic carbon nitride quantum dots for fluorescence determination of copper and silver ions and biothiols. Anal Chim Acta 1027: 121–129
50. Chen XX, Hong F, Zhang WL, Wu DZ, Li TH, Hu FT, Gan N, Lin JY, Wang QQ (2019) Microchip electrophoresis based multiplexed assay for silver and mercury ions simultaneous detection in complex samples using a stirring bar modified with encoded hairpin probes for specific extraction. J Chromatogr A 1589:173–181
51. Ye F, Liang XM, Xu KX, Pang XX, Chai Q, Fu Y (2019) A novel dithiourea-appended naphthalimide "on-off" fluorescent probe for detecting Hg^{2+} and Ag^{+} and its application in cell imaging. Talanta 200:494–502
52. Safavi A, Ahmadi R, Mohammadpour Z (2017) Colorimetric sensing of silver ion based on anti aggregation of gold nanoparticles. Sensor Actuat B-Chem 242:609–615
53. Kim JH, Kim KB, Park JS, Min N (2017) Single cytosine-based electrochemical biosensor for low-cost detection of silver ions. Sensor Actuat B-Chem 245:741–746
54. Zhao XE, Lei CH, Gao Y, Gao H, Zhu SY, Yang X, You JM, Wang H (2017) A ratiometric fluorescent nanosensor for the detection of silver ions using graphene quantum dots. Sensor Actuat B-Chem 253:239–246
55. He LY, Lu YX, Wang FY, Jing WJ, Chen Y, Liu YY (2018) Colorimetric sensing of silver ions based on glutathione-mediated MnO_2 nanosheets. Sensor Actuat B-Chem 254:468–474
56. Shahamirifard SA, Ghaedi M, Hajati S (2018) A new silver (I) ions optical sensor based on nanoporous thin films of sol-gel by rose bengal dye. Sensor Actuat B-Chem 259:20–29
57. Zhang YW, Ye AY, Yao YW, Yao C (2019) A sensitive near-infrared fluorescent probe for detecting heavy metal Ag^{+} in water samples. Sensors 19:247
58. Muhlradt PF, Kie BM, Meyer H (1997) Isolation, structure elucidation, and synthesis of a macrophage stimulatory lipopeptide from mycoplasma fermentans acting at picomolar concentration. J Exp Med 185:1951–1958
59. Fields GB, Nobel RL (1990) Solid phase peptide synthesis utilizing 9-fluorenylmethoxycarbonyl amino acids. Int J Pept Protein Res 35: 161–214
60. Liu ZP, He WJ, Guo Z (2013) Metal coordination in photoluminescent sensing. Chem Soc Rev 42:1568–1600
61. Godwin HA, Berg JM (1996) A fluorescent zinc probe based on metal-induced peptide folding. J Am Chem Soc 118:6514–6515
62. US Environmental Protection Agency, EPA Office of Water, Washington, DC. https://www.epa.gov/ground-water-and-drinking-water/national-primary-rinking-water-regulations, EPA 816-F- 09-0004, May 2009